RESEARCH ARTICLE

Oral Dosing of Chemical Indicators for *In Vivo* Monitoring of Ca^{2+} Dynamics in Insect Muscle

Ferdinandus[1], Satoshi Arai[2], Shin'ichi Ishiwata[2,3,4], Madoka Suzuki[2,3], Hirotaka Sato[1]*

1 School of Mechanical and Aerospace Engineering, Nanyang Technological University, Singapore, Singapore, 2 WASEDA Bioscience Research Institute in Singapore (WABIOS), Singapore, Singapore 3 Organization for University Research Initiatives, Waseda University, Tokyo, Japan, 4 Department of Physics, Faculty of Science and Engineering, Waseda University, Tokyo, Japan

* hirosato@ntu.edu.sg

Abstract

This paper proposes a remarkably facile staining protocol to visually investigate dynamic physiological events in insect tissues. We attempted to monitor Ca^{2+} dynamics during contraction of electrically stimulated living muscle. Advances in circuit miniaturization and insect neuromuscular physiology have enabled the hybridization of living insects and man-made electronic components, such as microcomputers, the result of which has been often referred as a Living Machine, Biohybrid, or Cyborg Insect. In order for Cyborg Insects to be of practical use, electrical stimulation parameters need to be optimized to induce desired muscle response (motor action) and minimize the damage in the muscle due to the electrical stimuli. Staining tissues and organs as well as measuring the dynamics of chemicals of interest in muscle should be conducted to quantitatively and systematically evaluate the effect of various stimulation parameters on the muscle response. However, existing staining processes require invasive surgery and/or arduous procedures using genetically encoded sensors. In this study, we developed a non-invasive and remarkably facile method for staining, in which chemical indicators can be orally administered (oral dosing). A chemical Ca^{2+} indicator was orally introduced into an insect of interest via food containing the chemical indicator and the indicator diffused from the insect digestion system to the target muscle tissue. We found that there was a positive relationship between the fluorescence intensity of the indicator and the frequency of electrical stimulation which indicates the orally dosed indicator successfully monitored Ca^{2+} dynamics in the muscle tissue. This oral dosing method has a potential to globally stain tissues including neurons, and investigating various physiological events in insects.

Introduction

The fusion of microcomputers and living insects, resulting in Cyborg Insects, also known as Insect–Machine Hybrid Systems or Living Machines [1], which include biological actuators and biological machines, has been a popular research topic owing to the production of miniature

Competing Interests: The authors have declared that no competing interests exist.

digital circuits and study of insect neuromuscular physiology [2, 3]. Ultra-small, radio-enabled, neuromuscular recorders and stimulators have been designed and manufactured to measure EMG (electromyogram) and to induce certain motor actions even in untethered and free flight situations [3–17]. Most attempts toward Cyborg Insects were to find which muscular or neural sites should be stimulated to induce a specific motor action and by what electrical signals (amplitude, frequency, and waveform). A challenge that remains is to regulate the induced motion to draw a user-determined path in a feedback controlled manner, where motor actions are appropriately graded by altering certain stimulation parameters [14]. To develop a model based feedback control system, we need to quantitatively investigate the effect of a given parameter on motor actions. To this end, it is desirable to visualize the muscle contractions, in other words, to monitor the dynamics of the intracellular Ca^{2+} levels (a significant second messenger molecule for muscle contraction) *in vivo* during electrical stimulation.

In vivo bioimaging is a promising way to gain insights into the physiological effects of exogenously applied electrical stimuli on living muscles. Advances in microscopic technology and the development of fluorescence labeling technology enable us to observe the dynamics of signaling molecules and intracellular components at cellular and tissue levels [18]. In particular, recent advances in the development of fluorescence imaging techniques provide various tools to visualize the dynamics of Ca^{2+}, an ion widely considered to be a significant second messenger molecule.

Ca^{2+} dynamics in living muscle cells are key factors for understanding muscular physiology. The sarcoplasmic reticulum (SR) releases Ca^{2+} to bind with troponin and alter the configuration of tropomyosin, which then allows the formation of cross-bridges between actin and myosin filaments to enable muscle contraction [19, 20]. Gordon and Dickinson reported the active role of Ca^{2+} in controlling the mechanical power output from flight muscles in *Drosophila melanogaster* [21]. Since Ca^{2+} is a major regulator for the motor action of muscle cells, we were motivated to visualize and further characterize Ca^{2+} dynamics in muscles in order to develop stimulation protocols that would be able to reliably induce the desired motor actions, all with the aim of producing an advanced level Cyborg Insect. Ca^{2+} imaging is a key technology not only for the study of muscular physiology in developing Cyborg Insects but also for a comprehensive physiological observation of the sensory units and the brain. Ca^{2+} imaging is popularly used in insect optophysiological studies to visualize neuronal activity in the antennal lobes of various insects. For instance, Joerges et al. [22] and Galizia and Kimmerle [23] utilized a confocal microscope to visualize Ca^{2+} dynamics representing the neuronal responses to a variety of odors in the glomerulus of the antennal lobes of honeybees. Wang et al. [24] employed a two-photon Ca^{2+} imaging technique to map out the glomerular activation evoked by different odors in the antennal lobe of flies. Overall, there are many great needs for Ca^{2+} imaging techniques in various insect neuromuscular physiology studies.

Two types of Ca^{2+} indicators (i.e. genetically encoded and chemical indicators) have been investigated, with each indicator presenting both advantages and disadvantages [25–27]. Genetically encoded indicators, such as Cameleon and GCaMP, use specifically designed vectors that contain special sequences that genetically target organelles and tissues of interest. Although some biological laboratories employed these methods using transgenic animals [28, 29], the application of these methods are still limited to a few animal species, such as: mouse, fly, pig, and sheep, owing to the genetic complexity of the organism of interest [30]. A wide variety of chemicals to monitor Ca^{2+} concentrations without the needs for genetic modification have been synthesized to date. There are commercially available Ca^{2+} indicators with a wide range of Ca^{2+} affinities including Calcium Green-1, Fluo-3, Fluo-4, and Fluo-8. However staining living tissues and cells with chemical indicators presents its own challenges, especially in *in vivo* applications. Regularly employed protocols for *in vivo* staining with chemical

indicators need to immobilize the animal of interest and to excise and expose the target tissues in order to inject, drip or spray the chemicals. The target cells and tissues could be crucially damaged during such a staining process, especially for small animals like insects, which would consequently cause a significant physiological difference between the stained and intact animals.

Herein, we propose a non-invasive and facile method to load chemical indicators into the tissues of living insects via jelly (insect food) containing the chemical indicators of interest, which is subsequently fed to living insects. The chemical indicators are not injected into dissected tissues, but an intact insect is simply fed with the jelly to orally introduce the chemical indicators from the mouth to the fore-, mid-, and hindguts via the esophagus. In general, insects digest food in the midgut, in which macromolecules are broken down into smaller components for absorption in the mid- and hindguts. Unlike in vertebrates, once molecules are absorbed, they are circulated around the insect body through the flow of hemolymph (insect body fluid), which are then delivered into various insect tissues [19]. Similarly, chemical indicators for physiological investigations and experiments, such as the Ca²⁺ indicator, could be orally dosed and delivered to muscle tissues of living insects. In the present study, we developed and tested the oral dosing method by using a variety of chemical dyes and indicators. Unlike the more commonly used methods to load chemical indicators, the oral dosing method does not require anaesthetizing and immobilizing the animal, which can freely and naturally behave and feed during the dosing, loading, and staining periods.

After we examined a variety of chemical indicators for staining muscles via the oral dosing method, we chose a chemical Ca²⁺ indicator (Fluo-8) and a cell-staining chemical (Cell Tracker) to investigate the effect of exogenously applied electrical stimuli on the stained muscle. We then conducted *in vivo* monitoring of Ca²⁺ dynamics in insect muscles in response to electrical stimulus.

Materials and Methods

Study Animal

We used *Mecynorrhina torquata* (Coleoptera: Scarabaeidae) as our insect model. *Mecynorrhina torquata* beetles are approximately 60 mm long and 8 g weigh. The beetles were kept in separate plastic terrariums (20 cm × 15 cm × 15 cm) with tissue paper at the bottom and were fed with a cup of sugar jelly (Lai Bao Food Co., Ltd) every 2–3 days. The temperature and relative humidity in the terrariums were maintained at 23°C and 50%, respectively [10]. The use of beetles is permitted by the Agri-Food & Veterinary Authority of Singapore (AVA, HS code: 01069000, Product code: ALV002). Invertebrates including insects are exempt from the ethics for animal experimentation according to National Advisory Committee for Laboratory Animal Research (NACLAR) Guidelines.

Chemicals

Fluo-8, AM was acquired from AAT Bioquest, Inc. Cell Tracker Orange CMRA; Rhodamine 123; bis-(1,3-dibutylbarbituric acid) trimethine oxonol [DiBAC$_4$(3)] and Grace's insect medium (1X), unsupplemented, were obtained from Life Technologies. Rhodamine B was purchased from Sigma-Aldrich. Dimethyl sulfoxide (DMSO) was acquired from Kanto Chemical Co. Inc. Fluo-8, AM (50 µg), Cell Tracker Orange CMRA (50 µg), Rhodamine 123 (3 mg), and DiBAC$_4$(3) (5 mg) were each diluted with DMSO to produce 1 mM stock solutions. Rhodamine B (5 mg) was diluted in water to produce 1 mM stock solution.

Electrical Stimulation Apparatus and Fluorescence Microscopy

An Agilent 33220A 20-MHz function/arbitrary waveform generator was used to perform electrical stimulation. An Agilent DSO 1004A 60 MHz oscilloscope was used to monitor the waveform that was generated during stimulation. An Olympus MVX10 Macro Zoom System Microscope with an objective lens (MVPLAPO 1X, N.A. = 0.25) was used for observation. A BP460–480 excitation filter, a DM485 dichroic mirror, and a BA495–540 barrier filter were used to observe Fluo-8, Rhodamine 123, and DiBAC$_4$(3). A BP535–555HQ excitation filter, a DM565HQ dichroic mirror, and a BA570–625HQ barrier filter were used to observe Cell Tracker Orange CMRA and Rhodamine B. An Olympus 130 W U-HGLGPS light guide-coupled illumination system was used as the fluorescent light source. The optical filters, mirrors, and fluorescent light source were purchased from Olympus. An electron-multiplying charge-coupled device (EM-CCD) camera (iXon3 897; Andor Technology) and Andor iQ2.7 software (Andor Technology) were used to capture images. An external trigger device (ER-BOBD-100; Andor Technology) was used to record the electric stimulation that was triggered by the waveform generator. The size of the observation field was 4.1×4.1 mm in 512×512 pixels. Two-dimensional images were obtained with exposure time of 30 ms and time series images were acquired with a rate of 45–47 ms per frame, or approximately 22 Hz. Fig. 1 illustrates the experimental setup that was utilized in this study.

Oral Dosing of Chemical Indicators and Electrode Implantation

The beetles were fed with home-made jelly that contained the chemical indicators. The jelly was made from mixing 153.5 mg of extra fine caster sugar (SIS sugar) in 500 mL of deionized water and was heated until all of the sugar dissolved. Three grams of agar-agar (Jim Willie Trading Co.) was added to the sugar solution while the heat was maintained, and the mixture was then brought to a boil. Afterward, the heat was turned off, and the solution was cooled to room temperature. The jelly solution was then transferred to small containers and placed in the freezer to solidify. Once the jelly solidified, it was mechanically mashed into small pieces using a spoon prior to mixing with the chemical indicators. Stock solutions of chemical indicators were then mixed with the mashed jelly (1 mL) to produce a final concentration of 60 μM of indicator in the mixture. The beetles were then subsequently fed with the jelly mixture (60 μM, 1 mL) for 2 days. One chemical indicator is mixed in one jelly solution, except for Fluo-8 and Cell Tracker which were mixed together. After the beetle was fed with the mixed jelly for 2 days, it was fixed on a dissection plate using rubber bands, insect pins, and clay while leaving the leg of interest free (a micrograph in Fig. 1). A small observation area was made on the side of the femur to observe the flexion muscle. One microliter of Grace's insect medium was dropped to the opening to prevent drying of the observation area. The electrode used was a paraformaldehyde-coated thin silver wire that was acquired from A-M systems. The inserted portion of the silver wire was flamed to remove the insulation. The electrically stimulated sites were either on the right side of the muscle (S1B Fig.) or on the left side.

Data Acquisition, Electrical Stimulation, and Data Analysis

Once the beetle was set on the stage under the microscope, data acquisition was started by using the filter setting for the indicator of choice. To investigate the effect of electrical stimulus on Ca^{2+} concentration in muscle, the beetles which were fed with Fluo-8 and Cell Tracker-mixed jelly were further examined under electrical stimulation, and data was acquired as a set of time series images using Fluo-8 filter setting followed by another set of images using Cell Tracker filter setting with 5–10 minutes time interval between each acquisition. Electrical stimulation began with multiple-pulse trains (50 Hz, 10% duty cycle, 2 V) for 3 seconds at 10
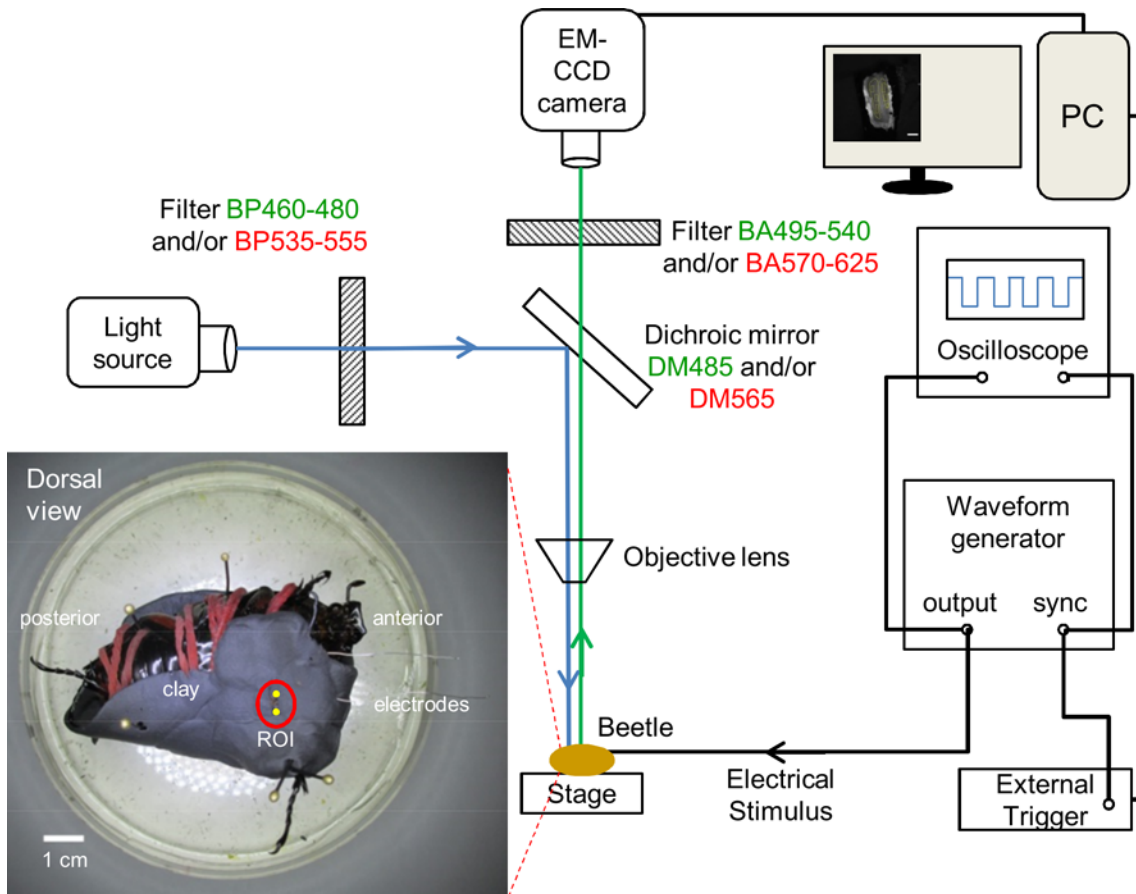
Figure 1. Illustration of fluorescence microscopy and electrical stimulation setups. The filter and mirror set in green font is used to observe Fluo-8, Rhodamine 123, and DiBAC$_4$(3). The filter and mirror set in red font is used to observe Cell Tracker and Rhodamine B. *Inset*, dorsal view of the beetle fixed upside down on dissection plate using clay, rubber bands (in red), and insect pins. Two PFA-coated thin silver wire electrodes (one working electrode and one counter electrode) were inserted into the ends of the muscle that are marked by 2 yellow dots. The insertion depth is approximately 2 mm, as measured from the outer cuticle. The red circle indicates the observation window that was used to observe the flexion muscle, which located inside the femur of the beetle leg.

second timestamp, and then followed with varying stimulation frequencies to complete one stimulation cycle. A stimulation cycle is defined as a set of varying frequencies of multiple-pulse trains (50 Hz, 10 Hz, 1 Hz, 100 Hz, 1 Hz and 50 Hz with constant 10% duty cycle, 2 V) applied for 3 seconds for each frequency and 27 seconds resting time (no stimulation) in between frequencies. One complete data acquisition of one stimulation cycle took about 3 minutes.

ImageJ software (National Institutes of Health) was used to analyze the images after capture. The fluorescence intensity of each dosed beetle leg was calculated from the average of the intensity measured from the two regions of interest (ROIs, S1A Fig.). These ROIs were chosen such that the center part of the leg, which is not part of the muscle, and the cuticles on the periphery, which give significantly higher fluorescence signal compared to the muscle, were excluded for analysis. For the purpose of measuring the fluorescence intensity change during electrical stimulation on beetle leg, the intensity was only measured at the ROI adjacent to the stimulated site (S1B Fig.).

Results and Discussion

Staining of Living Insect Leg Muscle with Orally Dosed Chemical Indicators

First, we tested dosing beetles with different chemical indicators to investigate the effectiveness of the novel oral-dosing method for in vivo staining. Insect has unique digestion and circulation systems in which the absorbed molecules from the guts are circulated around the body and directly can be distributed into tissues [19]. Thus our hypothesis is that these chemical indicators could be able to stain insect leg muscle by oral administration via food. The survivorship of the target animal, *M. torquata*, after the oral dosing of the tested chemical indicators was sufficient for our purposes. All of the beetles that were fed with either Rhodamine B, Rhodamine 123, or DiBAC$_4$(3) [N = 5 beetles for each indicator] and 9 out of 10 beetles that were fed with the Fluo-8 and Cell Tracker mixed jelly were still active for at least 1 week from the start of oral dosing.

The average fluorescence intensity of all the beetle legs (N = 5 beetles, n = 30 beetle legs for control, DiBAC$_4$(3), Rhodamine B, and Rhodamine 123; N = 9 beetles, n = 30 beetle legs for Fluo-8 and Cell Tracker) was summarized in Fig. 2. Based on the fluorescence images and the digitized fluorescence intensities that are shown in Fig. 2, we found that the fluorescence intensity increased after oral dosing with all of the tested chemical indicators.

The control beetles were fed with as-is home-made jelly (no chemical indicators added) for 2 days prior to observation. The control beetles' legs exhibited a certain level of fluorescence intensity (auto-fluorescence), which might be attributed to the organelles that contain fluorescence-emitting molecules, such as NAD(P)H inside the mitochondria [31]. Among the tested chemical indicators, drastic increases in fluorescence intensity were observed for DiBAC$_4$(3) and Rhodamine B, while the intensity increases for Rhodamine 123, Fluo-8, and Cell Tracker were relatively small. The differences in fluorescence intensity increase may account for the amount of dye that is retained in the muscle, but we could not confirm this based on our results alone, because different dyes have different properties, such as quantum yields and cellular distribution, as discussed below.

Rhodamine B (QY = 0.65) and Rhodamine 123 (QY = 0.90) have similar high quantum yields in ethanol [32], but Rhodamine 123 showed a small increase in the intensity. This may be attributed to the self-quenching of Rhodamine 123 at higher concentrations, where the quenching mechanism is not yet known. Rhodamine 123 and Rhodamine B are both cationic fluorescent dyes that are localized to mitochondria or acidic organelles such as endosomes and lysosomes, respectively [33–35].

DiBAC$_4$(3) is a bis-oxonol, slow-response potential indicator that is lipophilic, negatively charged, and binds to intracellular proteins or membranes of depolarized cells. DiBAC$_4$(3) was bright under observation, which was probably due to its properties, of which the quantum yield in aqueous solution is greatly increased once it binds to cytosolic proteins inside of the cell [18, 36–41].

Fluo-8 is a visible light-excitable Ca^{2+} indicator that has a K$_d$ for Ca^{2+} of approximately 389 nM with ex/em wavelengths at 490/514 nm, respectively [42, 43]. Fluo-8 has a low quantum yield of 0.16, as measured in 5 mM calcium citrate [44], and thus may appear less bright than the other high quantum yield indicators. Since Fluo-8 binds to intracellular Ca^{2+}, monitoring the fluorescence intensity of Fluo-8 would allow us to quantitatively track Ca^{2+} dynamics that are associated, for example, with muscle contraction, which can be induced by electrical stimulation. However, in general, the fluorescence intensity reflects not only the concentration of free Ca^{2+} ([Ca^{2+}]) but also the sample's displacement perpendicular to the focal plane of the microscope.
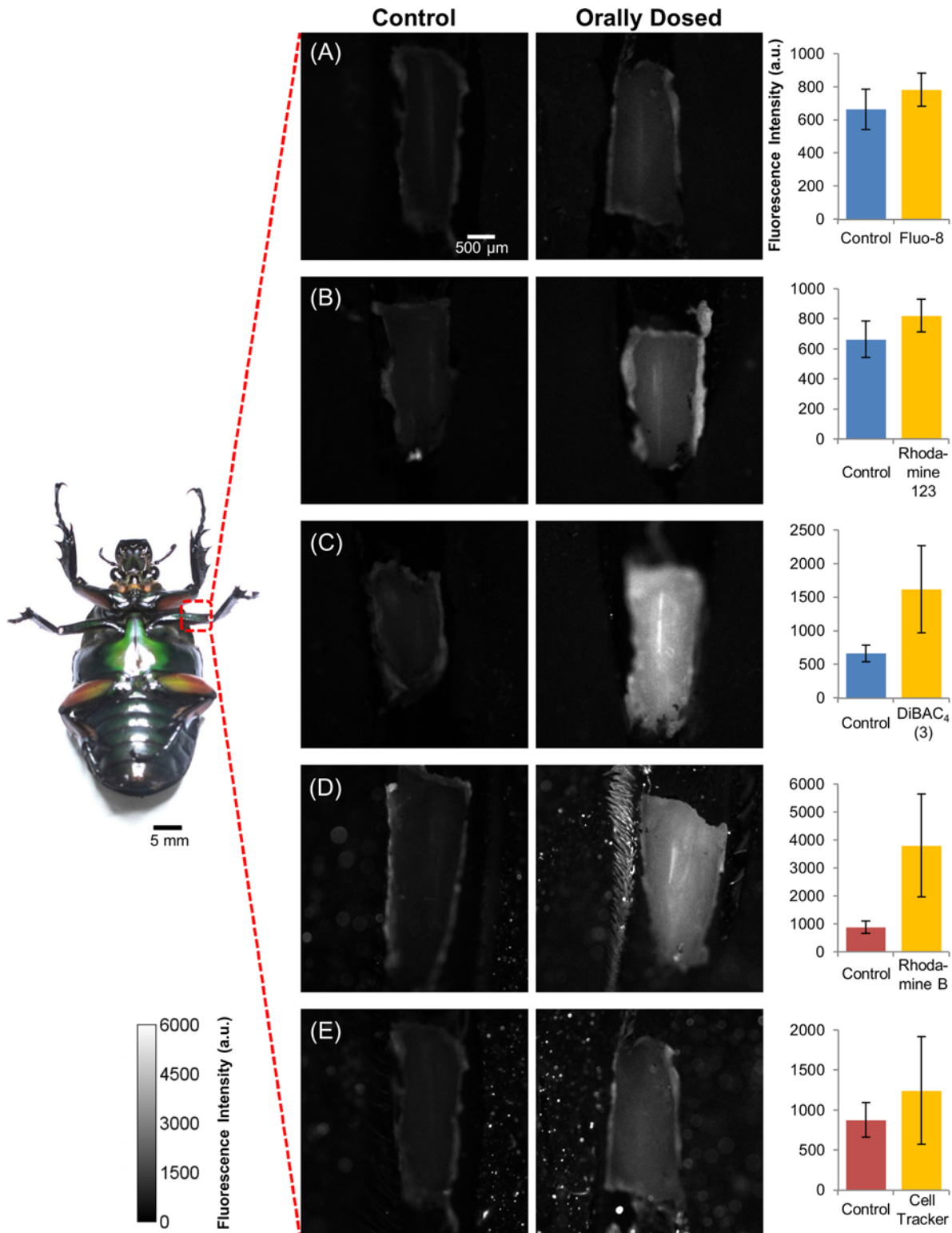
Figure 2. Difference in fluorescence intensity of insect flexion leg muscles of the control beetle and the beetle after oral dosing with chemical indicators. (A) Fluo-8; (B) Rhodamine 123; (C) DiBAC$_4$(3); (D) Rhodamine B; and (E) Cell Tracker. The Fluo-8, Rhodamine 123, and DiBAC$_4$(3) dosed beetle leg was observed under 460–480 nm excitation light and fluorescence emitted was collected within 495–540 nm. The Rhodamine B and Cell Tracker dosed beetle leg was observed under 535–555 nm excitation light and fluorescence emitted was collected within 570–625 nm. Fluorescence intensity was measured at the 2 regions of interest (ROIs) shown in S1A Fig. The images obtained were digitized by ImageJ software, and the averaged intensity is shown

in each bar graph. The graphs in the right column show the fluorescence intensities of each beetle leg dosed with different chemical indicators (center) compared with the control (left) beetle leg. The control beetles were fed with the home-made jelly (no chemical indicator added) for 2 days prior to observation. The error bars represent the standard deviation (S.D.) (N = 5 beetles, n = 30 beetle legs for control, DiBAC$_4$(3), Rhodamine B, and Rhodamine 123; N = 9 beetles, n = 30 beetle legs for Fluo-8 and Cell Tracker). Each data set was compared with control leg data set by student's t-test (Fluo-8, p = 1.42×10^{-4}; Rhodamine 123, p = 4.65×10^{-5}; DiBAC$_4$(3), p = 6.26×10^{-9}; Rhodamine B, p = 1.15×10^{-9} and Cell Tracker, p = 7.10×10^{-3}). The color scale is given on the bottom left corner of the image. The increase in fluorescence intensity for the chemical indicator-dosed beetle compared with the control beetle indicates that the oral dosing method successfully administers and delivers various chemical indicators in order to label the beetle leg muscle.

Cell Tracker was employed as the reference indicator, and Cell Tracker and Fluo-8 were mixed together into a jelly to feed to test beetles. Cell Tracker is a chemical indicator that concentrates in the cytoplasm after penetrating the cell and exhibits fluorescence ex/em wavelengths at 548/576 nm, respectively [18].

In our study, Fluo-8 and Cell Tracker were initially modified with an acetoxymethyl (AM) ester group, which makes the molecules sufficiently hydrophobic so that they diffuse into cells through the plasma membrane. Once these molecules enter into the cell, the intracellular esterase cleaves the AM ester group by hydrolysis, leaving the main group of the indicator molecules [26, 27]. A possible reason for the relatively small increases in the fluorescence intensity for Fluo-8 and Cell Tracker compared with the other chemical indicators could be associated with the AM ester cleavage process as well as the low quantum yield of these dyes. Although ideally the AM ester group is only cleaved inside of the cell by intracellular esterase, the cleavage could also be induced by some extracellular esterase and/or even H$_2$O, which might have occurred during the course of delivery of the indicator molecules from the digestive system to the leg muscle cells. If such extracellular cleavage occurs, the indicator molecules (without the AM ester group) cannot penetrate the plasma membrane and thus a smaller quantity of indicator molecules in the cells occurs.

Ca²⁺ Dynamics Induced by Electrical Stimulation

The fluorescence intensities of both Fluo-8 and Cell Tracker in the leg of the beetles changed upon electrical stimulation. After the beetle was orally dosed with jelly containing Fluo-8 and Cell Tracker, electrical stimulus of multiple pulse trains (100 Hz, 10% duty cycle, 2 V) was applied to one of the leg muscles of the beetle. Representative pseudocolor fluorescence images and intensity profiles for Fluo-8 and Cell Tracker indicators before, during, and after applying the electrical stimulus are shown in Fig. 3. The Fluo-8 signal in Fig. 3B reveals that there was an increase in [Ca²⁺] owing to the electrical stimulus, and [Ca²⁺] increased and then settled a plateau until the stimulation ended, and then gradually declined afterward. However, muscle contraction displaces the muscle in the direction perpendicular to the focal plane of fluorescence microscope so that the changes in the fluorescence intensity correspond not only to the changes in the [Ca²⁺] but probably also to the displacement of muscle out of the focal plane. Cell Tracker, which is a chemical indicator that is insensitive to Ca²⁺, was employed to estimate the contribution of the muscle contraction (vertical displacement) to the change in fluorescence intensity. The relatively low increase in the fluorescence intensity that was observed with Cell Tracker as a reference (Fig. 3C and 3D) is attributable to the muscle displacement (S2B Fig.).

Increase in the fluorescence intensity of Fluo-8 when induced by electrical stimulation was enhanced with increased stimulus frequency, while there was less significant change in that of Cell Tracker, as shown in Figs.4 and 5. The contraction of most muscles is regulated by the rate of physiological neural signal input to the muscle: higher neural input induces larger muscle contraction (tonic contraction) [45, 46]. Similarly, a higher frequency of externally applied electrical stimulus to living muscle induces larger muscle contraction (summation or
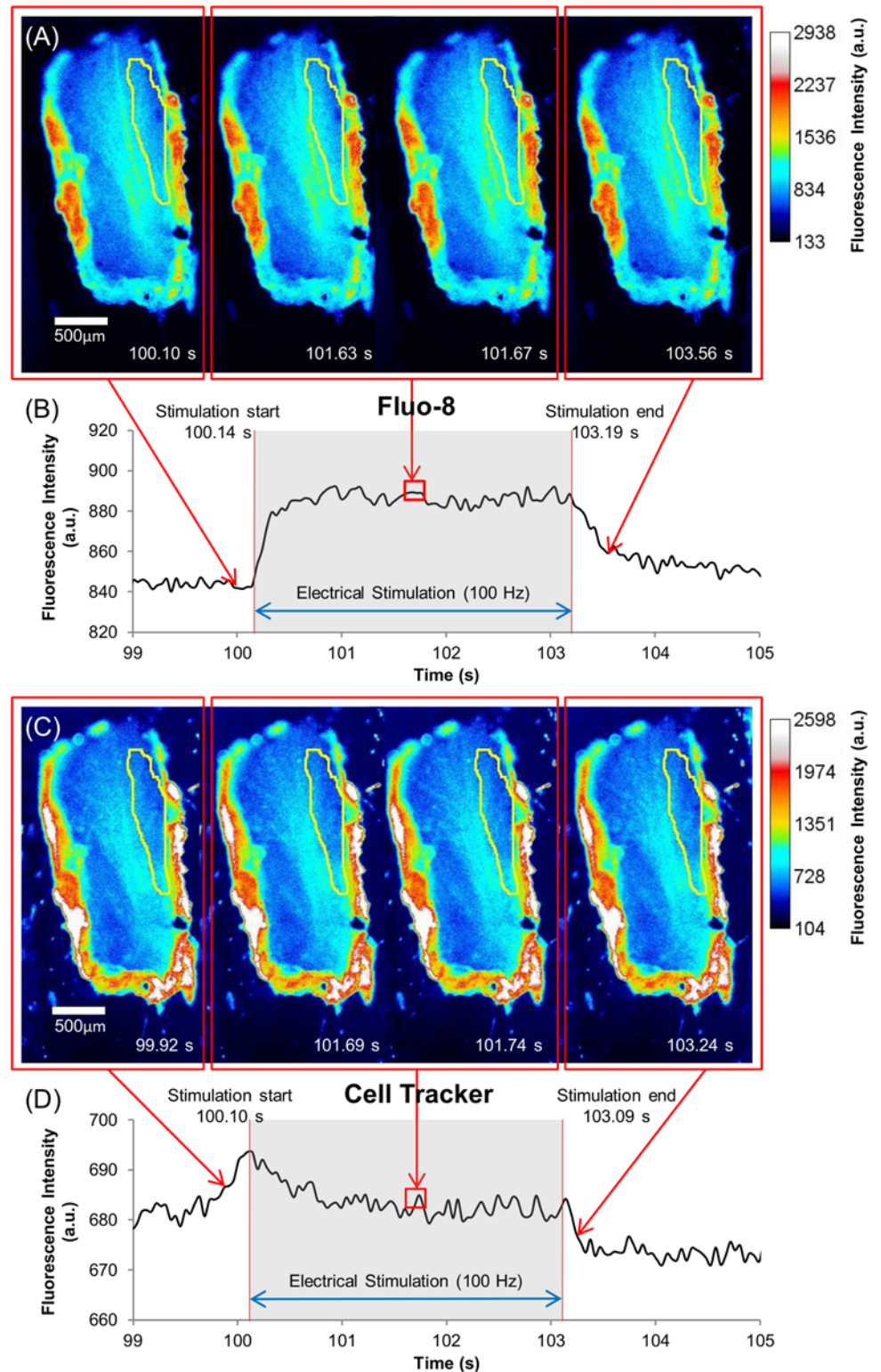
Figure 3. Ca²⁺ dynamics and muscle displacement of the beetle leg muscle under electrical stimulation with multiple pulse trains (100 Hz, 10% duty cycle, 2 V) for 3 s. Pseudocolor time series images of beetle leg muscle dosed with (A) Fluo-8 (60 μM) and (C) Cell Tracker (60 μM) indicators. ROIs are indicated by yellow region (as also shown in S1B Fig.). The color scale is given on the right side of each image (A) or (C) respectively. Fluorescence intensity dynamics of (B) Fluo-8 and (D) Cell Tracker under

electrical stimulation, digitized with ImageJ software from the ROI shown in (A) and (C) respectively. The stimulus timing is indicated by grey shading. The Fluo-8 pseudocolor images illustrate the fluorescence intensity dynamics that correspond to the Ca²⁺ dynamics inside the leg muscle: it increased at the start of electrical stimulation, was maintained during the application of the stimulus, and finally slowly decreased after the stimulus stopped. The Cell Tracker pseudocolor images display that the muscle displacement also causes intensity change during electrical stimulation, which slightly affects the Fluo-8 measurement.

facilitation) [47–49]. These two types of contraction-enhancement are both due to the elevation of [Ca²⁺] in muscle cells [19, 50]. Thus, we compared the dependency of fluorescence intensity changes ($\Delta F/F_0$ defined as below) of Fluo-8 and Cell Tracker on stimulation frequency in order to examine the effect of electrical stimulus on intracellular Ca²⁺ dynamics for each beetle leg. ΔF was defined by (F_1 —F_0), where F_1 is the average fluorescence intensity during stimulation and F_0 is that of 10 frames before beginning electrical stimulation, both measured from the ROI adjacent to the stimulated sites (electrode implanted sites) as shown in S1B Fig. To compare ΔF of these different chemical indicators, we evaluated the relative changes in ΔF, defined as $\Delta F/F_0$, at each stimulation frequency. The $\Delta F/F_0$ was then plotted with respect to applied stimulus frequencies in Fig. 4E. Note that the $\Delta F/F_0$ of Cell Tracker in some cases displays negative values; for example, during the 100 Hz stimulation and the second 1 Hz stimulation in Fig. 4E, indicating that the muscle displacement in some cases caused decreased intensity.

The $\Delta F/F_0$ of Fluo-8 depended on stimulus frequency, while the $\Delta F/F_0$ of Cell Tracker was relatively constant throughout the applied stimulus frequencies (Fig. 5A). Besides, such a distinguishable difference in the stimulation-frequency dependency of $\Delta F/F_0$ between Fluo-8 and Cell Tracker is not seen for the control beetle (Fig. 5B). Overall, these results indicate that the orally dosed Fluo-8 successfully monitored [Ca²⁺] inside the cell, and the change in the fluorescence intensity of Fluo-8 primarily reflects Ca²⁺ dynamics, whereas the muscle displacement has a rather small contribution to the intensity change.

Periodic fluctuations in fluorescence intensities of both Fluo-8 and Cell Tracker were continuously observed, regardless of applied electrical stimulations (Fig. 4B and 4D). The frequency of the periodic fluctuations was 0.25–0.26 Hz, which is similar to the frequency of tracheal respiration in beetles [51]. The tracheal respiration to supply oxygen caused periodic change in the leg muscle displacement, which resulted in the periodic fluctuations in the fluorescence intensity.

We found that the dependence of the [Ca²⁺] (monitored as Fluo-8 intensity change) on stimulation frequency is reproducible, as shown in Fig. 5. For example, the ΔF for the first 50 Hz stimulation (point 1) was reproduced on the last 50 Hz stimulation (point 6), although the muscle experienced different stimulation frequencies in between. This reproducibility indicates that the stimulated muscle was not significantly damaged and it can retain its elasticity and tension, although various stimulation frequencies were applied. Therefore, our stimulation protocol is fairly safe to use repeatedly on *M. torquata* beetles.

The challenge ahead is to substantially increase the fluorescence intensity of Fluo-8 than that of the auto-fluorescence in order to globally measure (visualize) and map out the Ca²⁺ dynamics over the whole muscle. Oral dosing of Fluo-8 in insect leg muscle allowed us to quantitatively estimate the effect of electrical stimulation on Ca²⁺ dynamics (muscle contraction) and observe whether the stimulated muscle has been damaged. However, the fluorescence intensity of Fluo-8 using the current oral dosing method is not sufficient to map out the Ca²⁺ dynamics over the whole muscle, because the auto-fluorescence level is high. We need to modify the oral dosing protocols and modify the molecular structure of the Ca²⁺ indicator such that it resists esterase cleavage, which occurs by hydrolysis, during the transport from the digestive system to the target muscle such that higher quantities of these indicators could diffuse into muscle cells.
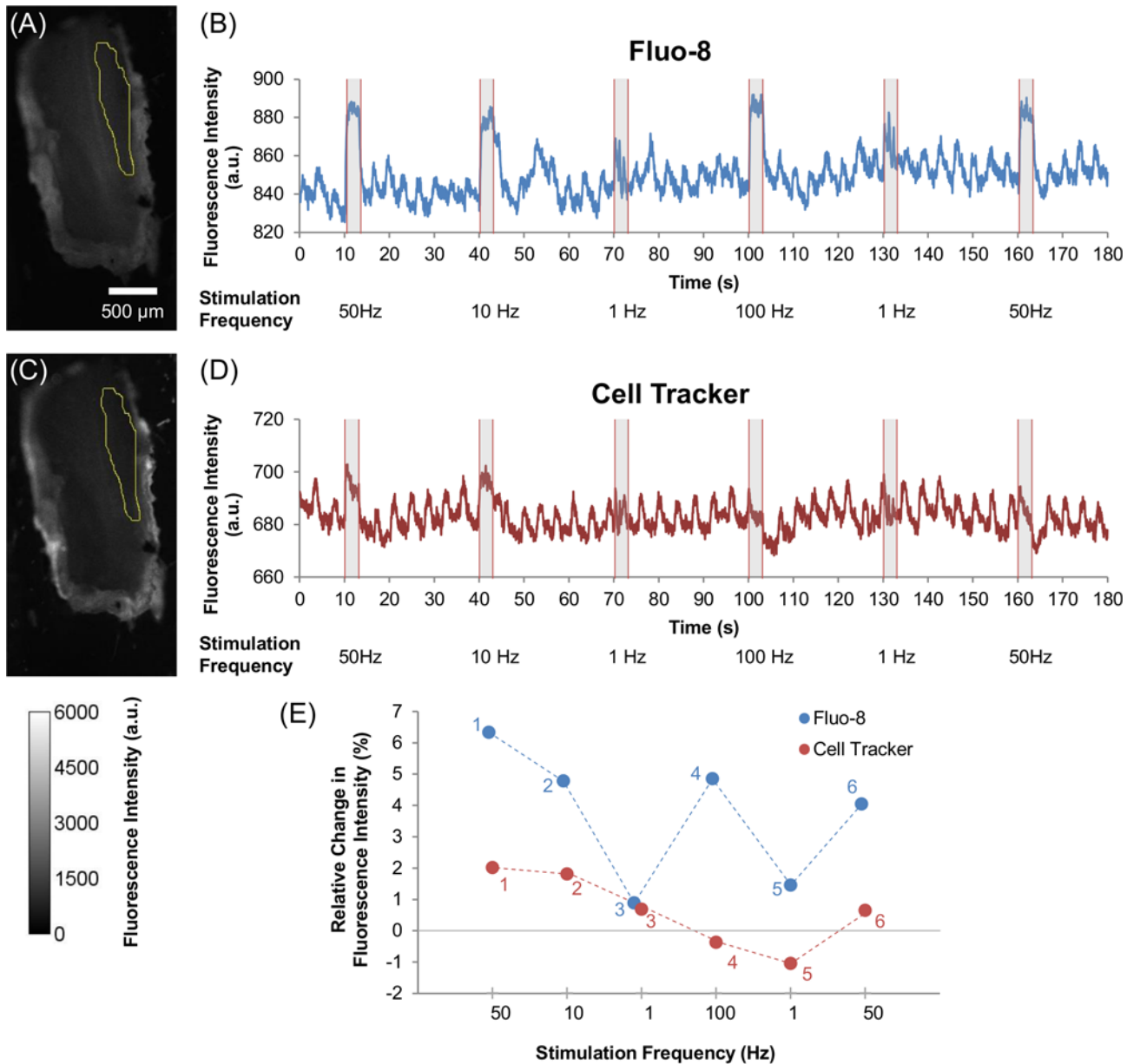
Figure 4. Effect of various electrical stimulation frequencies on Ca^{2+} dynamics and muscle displacement in beetle leg muscle. Images of beetle leg muscle that was dosed with (A) Fluo-8 (60 µM) and (C) Cell Tracker (60 µM), with the yellow selection indicating the ROI that was used for analysis (as also shown in S1B Fig.). The color scale is given at the bottom left corner of the image. Representative time courses showing the fluorescence intensity dynamics of (B) Fluo-8, and (D) Cell Tracker under various electrical stimulations of multiple pulse trains (50 Hz, 10 Hz, 1 Hz, 100 Hz, 1 Hz, and 50 Hz; 10% duty cycle; 2 V) observed from the ROI that are displayed in (A) and (C) respectively. All electrical stimulations were applied for 3 seconds periods with a 27 seconds resting period in between stimulations. The stimulus timing is indicated by grey shading. (E) Relative change in fluorescence intensity (($\Delta F/F_0$)×100%) for Fluo-8 (blue) and Cell Tracker (red) under varying electrical stimulation frequencies (50 Hz, 10 Hz, 1 Hz, 100 Hz, 1 Hz, and 50 Hz; 10% duty cycle; 2 V). The small numbers next to each plot indicate the order of stimulation; i.e., first from 50 Hz followed by varying frequency pulses (10 Hz, 1 Hz, 100 Hz, 1 Hz, and 50 Hz). The Fluo-8 intensity plot shows that Ca^{2+} dynamics are dependent on electrical stimulation frequency, whereas the Cell Tracker plot shows that the muscle displacement contributes a small amount.

doi:10.1371/journal.pone.0116655.g004
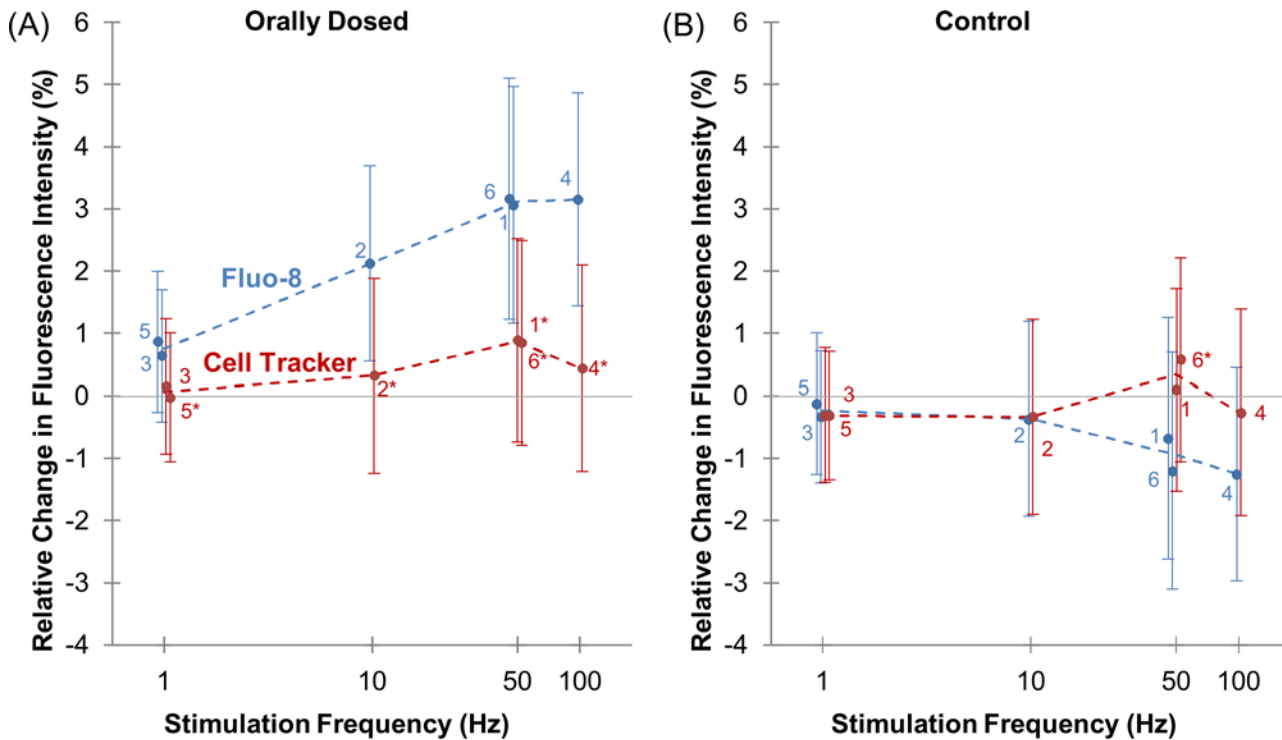
Figure 5. Relationship of Ca^{2+} dynamics with electrical stimulation frequency. Relative changes in fluorescence intensity (($\Delta F/F_0$)×100%) for leg muscle of (A) beetle orally dosed with Fluo-8 (blue) and Cell Tracker (red) and (B) control beetle measured with the filter setting used for Fluo-8 (blue) and Cell Tracker (red) under varying electrical stimulations (1 Hz, 10 Hz, 50 Hz, and 100 Hz; 10% duty cycle; 2 V). Data were analyzed from the ROI adjacent to the stimulated site (S1B Fig.). The error bars represent the S.D. (N = 8 beetles, n = 24 beetle legs for (A); N = 2 beetles, n = 8 beetle legs for (B)). The small numbers next to each plot indicate the order of stimulation. Cell Tracker data set was compared with Fluo-8 data set at each stimulation frequency evaluated by student's t-test both for dosed beetles in (A) (1st 50 Hz, $p = 9.37 \times 10^{-4}$; 10 Hz, $p = 7.45 \times 10^{-3}$; 1st 1 Hz, $p = 2.30 \times 10^{-1}$; 100 Hz, $p = 4.17 \times 10^{-4}$; 2nd 1 Hz, $p = 4.49 \times 10^{-2}$; and 2nd 50 Hz, $p = 8.16 \times 10^{-3}$) and for control beetles in (B) (1st 50 Hz, $p = 4.10 \times 10^{-1}$; 10 Hz, $p = 9.30 \times 10^{-1}$; 1st 1 Hz, $p = 9.29 \times 10^{-1}$; 100 Hz, $p = 5.69 \times 10^{-2}$; 2nd 1 Hz, $p = 6.85 \times 10^{-1}$; and 2nd 50 Hz, $p = 2.67 \times 10^{-2}$). The significant differences are displayed by an asterisk ($p < 0.05$). Fluo-8 intensity dynamics show that Ca^{2+} dynamics inside the muscle have a positive correlation with electrical stimulation frequency; i.e., higher stimulation frequency induces larger increase in [Ca^{2+}]. On the other hand, Cell Tracker intensity dynamics show that the frequency-dependent intensity change due to muscle displacement is not apparent.

doi:10.1371/journal.pone.0116655.g005

Summary

As a non-invasive and facile staining and labeling technique for insect bioimaging, we proposed and demonstrated oral dosing of chemical indicators by feeding live insects with jelly that contained the chemical indicators of interest. Insect leg muscles were successfully stained by orally dosed chemical indicators including Rhodamine B, Rhodamine 123, DiBAC$_4$(3), Fluo-8, and Cell Tracker Orange CMRA. The staining process in the oral dosing method does not require invasive and complicated operations and/or handling, unlike other conventional chemical dosing methods. The Ca^{2+} indicator Fluo-8 was further used to track Ca^{2+} dynamics, and Cell Tracker was used as reference to estimate the contribution of the displacement of electrically stimulated muscle to fluorescence intensity change owing to the displacement of the muscle. We confirmed that the fluorescence intensity increase of the orally dosed Fluo-8 was enhanced by increasing the frequency of electrical stimulus that was applied to the muscle, while that of the orally dosed Cell Tracker was slightly dependent on the stimulation frequency. This result indicates that the orally dosed Fluo-8 successfully monitored Ca^{2+} inside of the muscle cells. This method would allow us to quantitatively investigate the physiological effects of exogenously applied electrical stimulus on living insect muscles. The oral dosing method

would work to diffuse foreign materials and globally label molecules and tissues in varieties of insect species. Probably some messenger molecules in neurons in both motor units and sensory units can be labeled simultaneously. In the past years, researchers have been studying the relationship of the motor and sensory units in some insects, for example optic lobes and antennal lobes, in the central nervous system (CNS) of the insects of their interest [52–55]. The development of neuronal Ca²⁺ imaging enabled researchers to further examine the mechanism of neuronal and sensory Ca²⁺ signaling in some animals [56, 57]. Therefore, once the oral dosing method is modified and improved so as to non-invasively and globally but yet selectively stain specific motor and sensory units simultaneously, we can comprehensively investigate varieties of physiological events in CNS: we can study not only specific physiology of individual motor or sensory unit but also the connection and interactions (neural signal propagations) between these units.

Supporting Information

S1 Fig. Regions of interest (ROIs) used to analyze the data. Greyscale images of leg muscle with (A) 2 ROIs and (B) 1 ROI adjacent to the stimulated site. The center part of the leg which is not part of the muscle and the cuticles on the periphery was excluded from analysis. Two yellow dots in (B) indicate the position of the electrodes for stimulation. The stimulation site were either on the right side of the muscle, as depicted in (B) or on the left side of the muscle.
(TIF)

S2 Fig. Muscle displacement during electrical stimulation. (A) Yellow rectangle indicates the ROI used to draw a kymograph in (B). (B) Kymograph of muscle taken from the ROI shown in (A) for the time period (as in Fig. 3B) from 99.00 seconds to 105.00 seconds in which electrical stimulus (100 Hz; 10% duty cycle; 2 V) was applied from 100.14 seconds to 103.19 seconds as denoted by the two yellow lines.
(TIF)

Acknowledgments

Author Contributions

Conceived and designed the experiments: F SA SI MS HS. Performed the experiments: F SA MS HS. Analyzed the data: F SA MS HS. Wrote the paper: F SA SI MS HS.

References

1. Gross M (2013) Towards living machines. Curr Biol 23: R821–R823. doi: 10.1016/j.cub.2013.09.004 PMID: 24199226

2. Sato H, Maharbiz MM (2010) Recent developments in the remote radio control of insect flight. Front Neurosci 4. doi: 10.3389/fnins.2010.00199 PMID: 21629761

3. Holzer R, Shimoyama I (1997) Locomotion control of a bio-robotic system via electric stimulation. Proceedings of the 1997 IEEE/RSJ International Conference on Intelligent Robots and Systems, 1997 IROS'97. Grenoble: IEEE. pp. 1514–1519.

4. Ando N, Shimoyama I, Kanzaki R (2002) A dual-channel FM transmitter for acquisition of flight muscle activities from the freely flying hawkmoth, *Agrius convolvuli*. J Neurosci Methods 115: 181–187. doi: 10.1016/S0165-0270(02)00013-4 PMID: 11992669

5. Ando N, Kanzaki R (2004) Changing motor patterns of the 3rd axillary muscle activities associated with longitudinal control in freely flying hawkmoths. Zool Sci 21: 123–130. doi: 10.2108/zsj.21.123 PMID: 14993822

6. Fischer H, Ebert E (1999) Tegula function during free locust flight in relation to motor pattern, flight speed and aerodynamic output. J Exp Biol 202: 711–721. PMID: 10021324

7. Wang H, Ando N, Kanzaki R (2008) Active control of free flight manoeuvres in a hawkmoth, *Agrius convolvuli*. J Exp Biol 211: 423–432. doi: 10.1242/jeb.011791 PMID: 18203998

8. Maharbiz MM, Sato H (2010) Cyborg beetles. Sci Am 303: 94–99. doi: 10.1038/scientificamerican1210-94 PMID: 21141365

9. Bozkurt A, Gilmour RF, Lal A (2009) Balloon-assisted flight of radio-controlled insect biobots. IEEE Trans Biomed Eng 56: 2304–2307. doi: 10.1109/TBME.2009.2022551 PMID: 19692306

10. Sato H, Berry CW, Peeri Y, Baghoomian E, Casey BE, et al. (2009) Remote radio control of insect flight. Front Integr Neurosci 3: 24. doi: 10.3389/neuro.07.024.2009 PMID: 20161808

11. Daly DC, Mercier PP, Bhardwaj M, Stone AL, Aldworth ZN, et al. (2010) A pulsed UWB receiver SoC for insect motion control. IEEE J Solid-State Circuits 45: 153–166. doi: 10.1109/JSSC.2009.2034433

12. Hinterwirth AJ, Medina B, Lockey J, Otten D, Voldman J, et al. (2012) Wireless stimulation of antennal muscles in freely flying hawkmoths leads to flight path changes. PLoS One 7: e52725. doi: 10.1371/journal.pone.0052725 PMID: 23300751

13. Tsang WM, Stone AL, Aldworth ZN, Hildebrand JG, Daniel TL, et al. (2010) Flexible split-ring electrode for insect flight biasing using multisite neural stimulation. IEEE Trans Biomed Eng 57: 1757–1764. doi: 10.1109/TBME.2010.2041778 PMID: 20176539

14. Cao F, Zhang C, Doan TTV, Li Y, Sangi DH, et al. (2014) A Biological Micro Actuator: Graded and Closed-Loop Control of Insect Leg Motion by Electrical Stimulation of Muscles. PLoS One 9: e105389. doi: 10.1371/journal.pone.0105389 PMID: 25140875

15. Bozkurt A, Gilmour RF, Sinha A, Stern D, Lal A (2009) Insect–machine interface based neurocybernetics. IEEE Trans Biomed Eng 56: 1727–1733. doi: 10.1109/TBME.2009.2015460 PMID: 19272983

16. Kutsch W, Schwarz G, Fischer H, Kautz H (1993) Wireless transmission of muscle potentials during free flight of a locust. J Exp Biol 185: 367–373.

17. Fischer H, Kautz H, Kutsch W (1996) A radiotelemetric 2-channel unit for transmission of muscle potentials during free flight of the desert locust, *Schistocerca gregaria*. J Neurosci Methods 64: 39–45. doi: 10.1016/0165-0270(95)00083-6 PMID: 8869482

18. Johnson I, Spence MTZ (2010) The Molecular Probes handbook: A guide to fluorescent probes and labeling technologies. Life Technologies Corporation. 1060 p.

19. Chapman RF (1998) The insects: structure and function. New York: Cambridge university press. 770 p.

20. Szent-Györgyi A (1975) Calcium regulation of muscle contraction. Biophys J 15: 707–723. doi: 10.1016/S0006-3495(75)85849-8 PMID: 806311

21. Gordon S, Dickinson MH (2006) Role of calcium in the regulation of mechanical power in insect flight. Proc Natl Acad Sci U S A 103: 4311–4315. doi: 10.1073/pnas.0510109103 PMID: 16537527

22. Joerges J, Küttner A, Galizia CG, Menzel R (1997) Representations of odours and odour mixtures visualized in the honeybee brain. Nature 387: 285–288. doi: 10.1038/387285a0

23. Galizia CG, Kimmerle B (2004) Physiological and morphological characterization of honeybee olfactory neurons combining electrophysiology, calcium imaging and confocal microscopy. J Comp Physiol A 190: 21–38. doi: 10.1007/s00359-003-0469-0

24. Wang JW, Wong AM, Flores J, Vosshall LB, Axel R (2003) Two-photon calcium imaging reveals an odor-evoked map of activity in the fly brain. Cell 112: 271–282. doi: 10.1016/S0092-8674(03)00004-7 PMID: 12553914

25. Takahashi A, Camacho P, Lechleiter JD, Herman B (1999) Measurement of intracellular calcium. Physiol Rev 79: 1089–1125. PMID: 10508230

26. Paredes RM, Etzler JC, Watts LT, Zheng W, Lechleiter JD (2008) Chemical calcium indicators. Methods 46: 143–151. doi: 10.1016/j.ymeth.2008.09.025 PMID: 18929663

27. Russell JT (2011) Imaging calcium signals *in vivo*: a powerful tool in physiology and pharmacology. Br J Pharmacol 163: 1605–1625. doi: 10.1111/j.1476-5381.2010.00988.x PMID: 20718728

28. Miyawaki A, Griesbeck O, Heim R, Tsien RY (1999) Dynamic and quantitative Ca2+ measurements using improved cameleons. Proc Natl Acad Sci U S A 96: 2135–2140. doi: 10.1073/pnas.96.5.2135 PMID: 10051607

29. Tian L, Hires SA, Mao T, Huber D, Chiappe ME, et al. (2009) Imaging neural activity in worms, flies and mice with improved GCaMP calcium indicators. Nat Methods 6: 875–881. doi: 10.1038/nmeth.1398 PMID: 19898485

30. Houdebine LM (2002) The methods to generate transgenic animals and to control transgene expression. J Biotechnol 98: 145–160. doi: 10.1016/S0168-1656(02)00129-3 PMID: 12141984

31. Georgakoudi I, Jacobson BC, Müller MG, Sheets EE, Badizadegan K, et al. (2002) NAD(P)H and collagen as *in vivo* quantitative fluorescent biomarkers of epithelial precancerous changes. Cancer Res 62: 682–687. PMID: 11830520

32. Kubin RF, Fletcher AN (1983) Fluorescence quantum yields of some rhodamine dyes. J Lumin 27: 455–462. doi: 10.1016/0022-2313(82)90045-X

33. Ronot X, Benel L, Adolphe M, Mounolou J (1986) Mitochondrial analysis in living cells: the use of rhodamine 123 and flow cytometry. Biol Cell 57: 1–7. doi: 10.1111/j.1768-322X.1986.tb00458.x PMID: 2945606

34. Huang M, Camara A, Stowe D, Qi F, Beard D (2007) Mitochondrial inner membrane electrophysiology assessed by rhodamine-123 transport and fluorescence. Ann Biomed Eng 35: 1276–1285. doi: 10.1007/s10439-007-9265-2 PMID: 17372838

35. von Steyern FV, Josefsson JO, Tagerud S (1996) Rhodamine B, a fluorescent probe for acidic organelles in denervated skeletal muscle. J Histochem Cytochem 44: 267–274. doi: 10.1177/44.3.8648087

36. Epps DE, Wolfe ML, Groppi V (1994) Characterization of the steady-state and dynamic fluorescence properties of the potential-sensitive dye bis-(1, 3-dibutylbarbituric acid) trimethine oxonol (DiBAC$_4$(3)) in model systems and cells. Chem Phys Lipids 69: 137–150. doi: 10.1016/0009-3084(94)90035-3 PMID: 8181103

37. Klapperstück T, Glanz D, Klapperstück M, Wohlrab J (2009) Methodological aspects of measuring absolute values of membrane potential in human cells by flow cytometry. Cytometry Part A 75: 593–608. doi: 10.1002/cyto.a.20735

38. Yamada A, Gaja N, Ohya S, Muraki K, Narita H, et al. (2001) Usefulness and limitation of DiBAC$_4$(3), a voltage-sensitive fluorescent dye, for the measurement of membrane potentials regulated by recombinant large conductance Ca^{2+}-activated K$^+$ channels in HEK293 cells. The Japanese journal of pharmacology 86: 342–350. doi: 10.1254/jjp.86.342

39. González JE, Oades K, Leychkis Y, Harootunian A, Negulescu PA (1999) Cell-based assays and instrumentation for screening ion-channel targets. Drug Discov Today 4: 431–439. doi: 10.1016/S1359-6446(99)01383-5 PMID: 10461154

40. Bräuner T, Hülser DF, Strasser RJ (1984) Comparative measurements of membrane potentials with microelectrodes and voltage-sensitive dyes. BBA-Biomembranes 771: 208–216. doi: 10.1016/0005-2736(84)90535-2 PMID: 6704395

41. Plášek J, Sigler K (1996) Slow fluorescent indicators of membrane potential: a survey of different approaches to probe response analysis. J Photochem Photobiol B: Biol 33: 101–124. doi: 10.1016/1011-1344(96)07283-1

42. Piegari E, Lopez L, Ipiña EP, Dawson SP (2014) Fluorescence Fluctuations and Equivalence Classes of Ca2+ Imaging Experiments. PLoS One 9: e95860. doi: 10.1371/journal.pone.0095860 PMID: 24776736

43. Falk S, Rekling JC (2009) Neurons in the preBötzinger complex and VRG are located in proximity to arterioles in newborn mice. Neurosci Lett 450: 229–234. doi: 10.1016/j.neulet.2008.11.042 PMID: 19041367

44. AAT Bioquest Inc (2013) Physiological Probes & Assay Kits. Available:http://aatbio.com/catalog/PPAK.pdf. Accesed 2014 Jun 18.

45. Cornelius F (1982) Tonic contraction and the control of relaxation in a chemically skinned molluscan smooth muscle. J Gen Physiol 79: 821–834. doi: 10.1085/jgp.79.5.821 PMID: 6284861

46. May T, Brown B, Clements A (1979) Experimental studies upon a bundle of tonic fibres in the locust extensor tibialis muscle. J Insect Physiol 25: 169–181. doi: 10.1016/0022-1910(79)90096-9

47. Guschlbauer C, Scharstein H, Buschges A (2007) The extensor tibiae muscle of the stick insect: biomechanical properties of an insect walking leg muscle. J Exp Biol 210: 1092–1108. doi: 10.1242/jeb.02729 PMID: 17337721

48. Adrian E, Lucas K (1912) On the summation of propagated disturbances in nerve and muscle. J Physiol 44: 68–124. doi: 10.1113/jphysiol.1912.sp001503 PMID: 16993138

49. Orchard I, Lange AB (1986) Neuromuscular transmission in an insect visceral muscle. J Neurobiol 17: 359–372. doi: 10.1002/neu.480170502 PMID: 2877049

50. Titushkin IA, Rao VS, Cho MR (2004) Mode-and cell-type dependent calcium responses induced by electrical stimulus. IEEE Trans Plasma Sci 32: 1614–1619. doi: 10.1109/TPS.2004.832625

51. Westneat MW, Betz O, Blob RW, Fezzaa K, Cooper WJ, et al. (2003) Tracheal respiration in insects visualized with synchrotron X-ray imaging. Science 299: 558–560. doi: 10.1126/science.1078008 PMID: 12543973

52. Namiki S, Kanzaki R (2008) Reconstructing the population activity of olfactory output neurons that innervate identifiable processing units. Front Neural Circuits 2: 1. doi: 10.3389/neuro.04.001.2008 PMID: 18946541

53. Fox JL, Fairhall AL, Daniel TL (2010) Encoding properties of haltere neurons enable motion feature detection in a biological gyroscope. Proc Natl Acad Sci U S A 107: 3840–3845. doi: 10.1073/pnas. 0912548107 PMID: 20133721

54. Martin JP, Hildebrand JG (2010) Innate recognition of pheromone and food odors in moths: a common mechanism in the antennal lobe? Front Behav Neurosci 4. doi: 10.3389/fnbeh.2010.00159 PMID: 20953251

55. Webb B, Harrison RR, Willis MA (2004) Sensorimotor control of navigation in arthropod and artificial systems. Arthropod structure & development 33: 301–329. doi: 10.1016/j.asd.2004.05.009

56. Garaschuk O, Griesbeck O, Konnerth A (2007) Troponin C-based biosensors: A new family of genetically encoded indicators for *in vivo* calcium imaging in the nervous system. Cell Calcium 42: 351–361. doi: 10.1016/j.ceca.2007.02.011 PMID: 17451806

57. Grienberger C, Konnerth A (2012) Imaging calcium in neurons. Neuron 73: 862–885. doi: 10.1016/j. neuron.2012.02.011 PMID: 22405199